*Medical Infobahn for Europe*
*A. Hasman et al. (Eds.)*
*IOS Press, 2000*



# 3-D image analysis of abdominal aortic aneurysm

Marko Subasic and Sven Loncaric and Erich Sorantin*
*Faculty of Electrical Engineering and Computing, University of Zagreb*
*Unska 3, 10000 Zagreb, Croatia*
**Dept. of Radiology, University Hospital Graz, Auenbruggerplatz 34, A-8036, Austria*

**Abstract.** In this paper we propose a technique for 3-D segmentation of abdominal aortic aneurysm (AAA) from computed tomography (CT) angiography images. Output data form the proposed method can be used for measurement of aortic shape and dimensions. Knowledge of aortic shape and size is very important for selection of appropriate stent graft device for treatment of AAA. The technique is based on a 3-D deformable model and utilizes the level-set algorithm for implementation of the method. The method performs 3-D segmentation of CT images and extracts a 3-D model of aortic wall. Once the 3-D model of aortic wall is available it is easy to perform all required measurements for appropriate stent graft selection. The method proposed in this paper uses the level-set algorithm instead of the classical active contour algorithm developed by Kass et al. The main advantage of the level set algorithm is that it enables easy segmentation surpassing most of the drawbacks of the classical approach. In the level-set approach for shape modeling, a 3-D surface is represented by a real 3-D function or equivalent 4-D surface. The 4-D surface is then evolved through an iterative process of solving the differential equation of surface motion. Surface motion is defined by velocity at each point. The velocity is a sum of constant velocity and curvature-dependent velocity. The stopping criterion is calculated based on image gradient. The algorithm has been implemented in MATLAB and C languages. Experiments have been performed using real patient CT angiography images and have shown good results.

## 1. INTRODUCTION

Abdominal aortic aneurysm (AAA) [1], [2] is a cardiovascular disease that can be treated by open surgery or by placement of aortic stent graft. The main disadvantage of open surgery treatment is the invasive nature of the procedure. For this reason, an alternative procedure has been proposed recently that is based on endovascular placement of aortic stent graft through a minimally invasive opening on the patient body. However, the difficulty with this method is that accurate measurements of AAA must be made prior to the surgical procedure in order to choose the stent graft device of appropriate shape and size. A number of different modalities have been used for imaging of AAA, such as ultrasound, digital subtraction angiography (DSA), CT angiography, and contrast-agent enhanced MR angiography [3]. Modern medical imaging techniques followed by appropriate image analysis methods [4] have shown to be useful for measurements of AAA [5], [6].

In this paper, we describe a 3-D image analysis technique for segmentation of AAA from CT angiography images. The technique is based on 3-D deformable model and utilizes a level-set algorithm for implementation of the method. The method performs 3-D segmentation of CT images and extracts a 3-D model of aortic wall. Once the 3-D model of aortic wall is available, it is easy to perform all required measurements for appropriate stent graft selection. In our previous work [6], we have developed a semi automatic 3-D technique for aneurysm segmentation that is based on 2-D active contours with additional forces introduced for 3-D interaction between the slices. The method uses the classical active contour algorithm developed by Kass et al. [7]. The method proposed in this paper uses the level-set algorithm [10] instead of the classical active contour algorithm.

## 2. LEVEL-SET METHOD FOR DEFORMABLE MODEL-BASED SEGMENTATION

Deformable models have shown to be a powerful tool for medical image segmentation [8]. The original active contour algorithm [7] uses active contours (snakes). This classical snake approach has several disadvantages: (i) difficulties with segmentation of topologically complex structures, and (ii) complex implementation in 3-D. To overcome these difficulties, the level set method has been proposed [9], [10]. In this section, we will give a short description of level-set method in 2-D segmentation. Extension to three-dimensional case, which we use, is straightforward.

In this approach for shape modeling, a 2-D curve $\gamma$ is represented by a 3-D surface $\Psi$. The value of the $\Psi$ surface at some point $x$ is defined as a distance $d$ of the point $x$ to the 2-D curve $\gamma$ according to Equation 1.

$$\Psi(x,t=0)=\pm d \tag{1}$$

where $x\in\mathbf{R}^2$ are points in image space. The sign in Equation 1 determines whether the point lies outside or inside the 2-D curve $\gamma(t=0)$. In this manner, $\gamma$ is represented by the zero level set $\gamma(t)=\{x\in\mathbf{R}^2 \mid \Psi(x,t)=0\}$ of the level set function. The level set method then evolves the 3-D surface $\Psi$ instead of the original 2-D curve. The motion of $\Psi$ is described by means of a partial differential equation (PDE) shown in Equation 2.

Trading moving curve for moving surface makes things more complex, but the level-set method introduces some new qualities and resolves some problems found in the classical snake method. An important property of the level-set method is that as long as the surface stays smooth, its zero level set can take any shape, change topology, brake and merge. Another advantage is that it is easy to build accurate numerical schemes to approximate the equations of motion.

The evolution PDE for evolution of the function $\Psi(x,t)$ has the following form:

$$\frac{\partial\Psi(x,t)}{\partial t}+F\left|\nabla\Psi\right|=0 \tag{2}$$

with a given initial condition $\Psi(x, t=0)$. For numerical solution of the Equation 2 it is necessary to perform discretization in both space and time domains. For this purpose we discretize space coordinates using a uniform mesh of spacing $h$, with grid nodes denoted by indices $ij$. Let $\Psi_{ij}^{n}$ be the approximation to the solution $\Psi(ih,jh,n\Delta t)$, where $\Delta t$ is the time step. The expression for $\Psi_{ij}^{n+1}$ can be derived using the upwind finite difference method which gives us the final iteration expression in Equation 3.

$$\Psi_{ij}^{n+1}=\Psi_{ij}^{n}-\Delta tF\left|\nabla_{ij}\Psi_{ij}^{n}\right| \tag{3}$$

The speed term $F$ depends on the curvature $K$ and is separated into a constant advection term $F_0$ and the remainder $F_1(K)$, that is

$$F(K)=F_0+F_1(K) \tag{4}$$

The advection term $F_0$ defines a uniform direction speed of front, which corresponds to inflation force in classical snake models. The diffusion term $F_1(K)$ depends on the local curvature and smoothes out regions of high curvature thus corresponding to internal force in classical snake models. We use the following expression for the speed term

$$F = 1 - \varepsilon K \tag{5}$$

where ε is the entropy condition which regulates the smoothness of the curve .The proposed range for ε is 0.5 to 1.0.

The curvature is obtained from the divergence of the gradient of the unit normal vector to front, that is

$$K = \nabla \frac{\nabla \Psi}{|\nabla \Psi|} = \frac{\Psi_{xx}\Psi_y^2 - 2\Psi_x\Psi_y\Psi_{xy} + \Psi_{yy}\Psi_x^2}{(\Psi_x^2 + \Psi_y^2)^{3/2}} \tag{6}$$

In order to segment images the speed function $F$ also has to have an image based condition, which would cause propagating front to stop near desired object boundary. Multiplying the speed function $F$ with a quantity $k$ provides needed influence of image gradient. The term $k$ can be defined in several ways and we use the following form.

$$k(x, y) = e^{-|\nabla G_\sigma * I(x,y)|} \tag{7}$$

where $G_\sigma*I$ denotes image convolved with Gaussian smoothing filter whose characteristic width is σ.

We use the narrow band extension as proposed by Sethian et al. [10] where the front is moved by updating the level-set function only at a small set of points in the neighborhood of zero level-set called the narrow band. Two boundary curves of the narrow band are $\delta$ apart. During a given time step the value of $\Psi$ outside the narrow band is stationary and zero level-set cannot move past the narrow band. After a given number of iterations the curve $\gamma$, the level-set function, and the new narrow band are recalculated. We then calculate image-based term only inside narrow band and each $\Psi$ point have image-based term based on its corresponding Gaussian gradient point.

In the above text, we have described the level set method for segmenting two-dimensional images. Extension to three dimensions is straightforward by extending the array structures and gradient operators. In that case, $\Psi$ is a 4-D surface and we use the following expression for curvature of the level set function as stated in [9].

$$K = \frac{\Psi_{xx}(\Psi_y^2 + \Psi_z^2) + \Psi_{yy}(\Psi_x^2 + \Psi_z^2) + \Psi_{zz}(\Psi_x^2 + \Psi_y^2) - 2\Psi_x\Psi_y\Psi_{xy} - 2\Psi_x\Psi_z\Psi_{xz} - 2\Psi_z\Psi_y\Psi_{zy}}{(\Psi_x^2 + \Psi_y^2 + \Psi_z^2)^{3/2}} \tag{8}$$

## 3. 3-D ABDOMINAL AORTIC ANEURYSM SEGMENTATION

We apply the level-set method to the problem of AAA segmentation. The input to the level-set algorithm in this case is a 3-D array of volumetric CT angiography data of the human abdomen. We perform manual extraction of the region of interest containing the AAA from the volumetric data. This step reduces memory requests thus decreasing execution time.

To segment aortic wall we perform two steps. In the first step, we segment the inner boundary of aorta while in the second step we segment the outer boundary.

For segmentation of the inner boundary of aorta, we use the basic 3D level-set algorithm described in the previous section. In order to use the 3D level-set algorithm, an initial surface has to be defined. We choose the initial surface $\gamma_{init}$ to be a sphere because of its simplicity. The sphere center and radius have to be defined manually by the user and it has to be placed so that it resides entirely inside the abdominal aorta. The algorithm described below then evolves the surface $\gamma$ until it stops changing. The outline of the algorithm is shown in Table 1.

Calculate initial surface $\gamma_{init1}$ and initial $\Psi_1$
**repeat**
    **for** i =1,...,$N_{iter1}$ **do**
        Execute iteration in Equation 4
    **end for**
    Recalculate surface $\gamma_1$
    Recalculate narrow band
    Reinitiate $\Psi_1$ in narrow band
**until** $\gamma_1$ stops changing

Table 1.The level set algorithm for abdominal aortic aneurysm segmentation.

The output of the algorithm is the final surface $\gamma_{end1}$ representing the internal boundary of the aorta. The final $\gamma_{end1}$ in the first step is used to produce initial conditions in second step: calculation of outer aortic boundaries.

The implementation of level-set algorithm for segmenting of inner aortic boundaries is straightforward because of the high contrast between aortic interior and aortic wall. This is due to angiography technique used for obtaining CT data. This however is not the case while segmenting outer aorta boundary. The main difficulty is that surrounding tissue has the same optical density as aortic wall and in several places, they are very close together, making it impossible to determine border between them. The Level-set algorithm can successfully deal with small contact areas thanks to its local curvature based speed term, but cannot stop propagation of zero level-set inside surrounding tissue where the contact area is very large. This and variations in aortic diameter along aorta and especially in aneurysm area led us to use the 2-D level-set method on each slice with an additional stopping criterion.

Initial curvature $\gamma_{init2}$ for the 2-D level-set method is chosen to be a circle. The circle's center is calculated as mid-point of final $\gamma_{end1}$ points in current slice from previous step. The radius from initial surface $\gamma_{init2}$ is chosen to be scaled mean radius of final $\gamma_{end1}$ points in current. Initial curvature is constructed this way because we presume that we are expanding initial circle into a larger shape similar to circle. Calculated center of initial curvature $\gamma_{init2}$ is therefore estimated center of final $\gamma_{end2}$. This way we reduce chances of level-set's propagation outside outer aortic borders before the additional stopping criterion is applied.

The additional stopping criterion is based on knowledge of general facts on aorta: aortic surface is smooth and round. One can than presume that outer aortic boundary has same characteristics in areas where it is not distinguishable. The additional stopping criterion is basically a curve based on evolving curve $\gamma_2$ at a point in time when predefined percent $M$ of $\gamma_2$ points has met outer aortic border. The stopping criterion curve is built in following way: central point $C_\gamma$ is calculated as mid-point of $\gamma_2$. Then distance $r$ from each $\gamma_2$ point from $C_\gamma$ is calculated. Predefined number of distances $r_\alpha$ is chosen based on corresponding point's angles. That $r_\alpha$*'s* are then transformed using Fourier transformation. We than eliminate higher frequency Fourier coefficients. Low frequency Fourier coefficients are then transformed back into distances $r_{ifi}$, which are then increased by some amount. Those $r_{ifi}$ produce stopping criterion curve. In this way the stopping criterion curve estimates aortic border where it is not distinguishable.

After the additional stopping criterion is calculated, evolving curvature $\gamma$ will stop at aortic borders and on additional stopping curve.

We use thresholded image for computing of image gradient so inner boundaries of aorta would not interfere with outer boundary segmentation. In addition, some modifications to basic speed term have to be made in order to more efficiently prevent propagation of front into surrounding tissue: constant speed term is decreased and influence of curvature term is increased. The modified algorithm (Table 2.) is run to segment outer aortic boundary.

**repeat** for all slices
  Calculate initial surface $\gamma_{init2}$ and initial $\Psi_2$
  **repeat**
    **for** i =1,...,$N_{iter2}$ **do**
      Execute iteration in Equation 4
    **end for**
    Recalculate surface $\gamma_2$
    Recalculate narrow band
    Reinitiate $\Psi_2$ in narrow band
    **if** $n_{stat}/n_{all}>M$ **then**
      Calculate additional stopping criterion
  **until** $\gamma$ stops changing

Table 2.The level set algorithm for abdominal aortic aneurysm segmentation.

An additional modification to the original level-set algorithm has been made in order to reduces the chances of level-set's propagation outside outer aortic borders. We modified the curvature calculation (Equation 6) so that in derivatives calculation, second neighbor points are used instead of immediate neighbor points. This is done because curves are represented in discretized form and in that form curves that are convex can become locally concave. If that were true, curvature speed term would produce wrong effect making the surface expand faster instead of slowing down its expansion.

After performing both steps in aortic segmentation we end up with 3-D model of abdominal aorta, on which measurements can be performed.

The major part of the algorithm has been implemented in MATLAB program package while the most computationally complex steps of recalculating $\gamma$, narrow band and reinitialization of $\Psi$, have been implemented in C programming language.

## 4. RESULTS AND DISCUSSION

The algorithm has been tested using CT angiography images of a real patient. Segmentation is performed on manually pre-selected volume. Values of numerical constants for segmenting of inner aortic boundary are as follows. $F_0$=1, ε=0 .9. Gaussian smoothing filter is σ=0 .9. The constant $N_{iter}$ which determines the number of inner loops in Table 1 and Table 2 is set to 4 and width of narrow band is δ=6. The gradient of input data in Equation 8 is normalized and multiplied with weight factor of 2 so that the stopping criterion could function.. For segmenting of outer boundaries we use following values: $F_0$=0.01, ε=1.

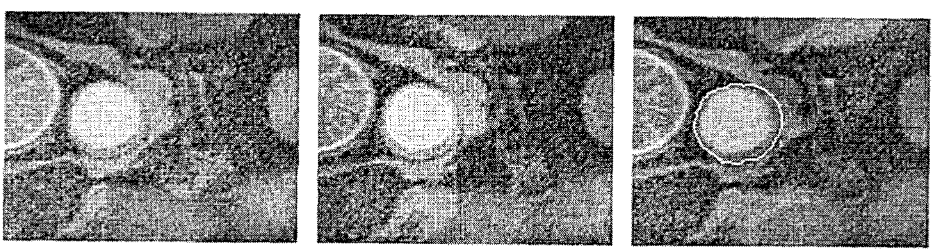

a) b) c)

Figure 1. Slice 11 (a) and slice with superimposed segmented aorta's inner (b) and outer (c) boundaries

a) b) c)

Figure 2. Slice 43 (a) and slice with superimposed segmented aorta's inner (b) and outer (c) boundaries

Figures 1 and 2 show the results of segmentation using the proposed algorithm. Subfigures a) show a slice of input data while subfigures b) and c) show segmented inner and outer aortic borders superimposed on the original slice.

## 5. CONCLUSION

Stent graft placement has been recently introduced as a method for less invasive treatment of abdominal aortic aneurysm. This technique requires accurate measurements of the aneurysm for selection of appropriate stent graft shape and size. These measurements are performed by imaging the patient using various medical imaging modalities. In this paper, we have presented a novel 3-D algorithm for abdominal aortic aneurysm segmentation from CT images. The algorithm uses a 3-D deformable model and is implemented using the level set algorithm. Experiments have been performed using CT images of patients having abdominal aortic aneurysm. Experiments have shown good results. Future work will include different approaches to computation of additional stopping criterion.

## 6. REFERENCES

[1] C. B. Ernst, "Abdominal aortic aneurysms", New England Journal of Medicine, vol.328, pp.1167 – 1172,1993.

[2] R. M. Berne and M. N. Levy, Cardiovascular Physiology, 7th Ed., Mosby-Year Book, 1997.

[3] S. A. Thurnher, R. Dorffner, M. M. Thurnher, F. W. Winkelbauer, G. Kretschmer, P. Polterauer, and J. Lammer, "Evaluation of abdominal aortic aneurysm for stent-graft placement: Comparison of Gadolinium-enhanced MR angiography versus helical CT angiography and digital subtraction angiography," Radiology ,vol.205,pp.341 –352,1997.

[4] A. P. Dhawan and S. Juvvadi, "Knowledge-based analysis and understanding of medical images," Computer Methods and Programs in Biomedicine, vol.33, pp.221 –239,1990.

[5] M. Garreau, J. L. Coatrieux, R. Collorec and C. Chardenon, "A knowledge-based approach for 3-D reconstruction and labeling of vascular networks from biplane angiographic projections, "IEEE Transactions on Medical Imaging ,vol.10,pp.122 –131,1991.

[6] S. Loncaric,D. Kovacevic and E. Sorantin, "Semi-automatic active contour approach to segmentation of computed tomography volumes, "in Proceedings of SPIE Medical Imaging ,2000, vol.3979,p.to be published.

[7] M. Kass, A. Witkin and D. Terzopoulos, "Snakes: active contour models, "International Journal of Computer Vision, vol. 1,pp.321 –331,1987.

[8] T. McInerey and D. Terzopoulos, "Deformable models in medical image analysis: A survey, "Medical Image Analysis, vol.1, pp. 91 –108,1996.

[9] S. Osher and J. A. Sethian, "Fronts propagating with curvature dependent speed: algorithms based on hamilton-jacobi formulation, "Journal of Computational Physics, vol.79, pp.12 –49,1988.

[10] R. Malladi, J. A. Sethian and B. C. Vemuri, "Shape modeling with front propagation, "IEEE Transactions on PAMI, vol.17, pp.158 –176,1995.